Romanian Reports in Physics, Vol. 65, No. 2, P. 427–436, 2013

MEASUREMENT OF THE DIFFRACTIVE DIS CROSS SECTION AT THE H1 EXPERIMENT*

N. RAIČEVIĆ, ON BEHALF OF THE H1 COLLABORATION

University of Montenegro, Faculty of Science, Džordža Vašingtona BB, 81000 Podgorica, Montenegro, E-mail: raicevic@mail.desy.de

Received September 12, 2012

Abstract. The most recent measurements of the diffractive deep-inelastic scattering cross section obtained with the H1 detector are reported. Measurements are performed using two approaches. One approach is based on detection of the diffractive processes ep → eXY where Y denotes a proton or its low mass excitation with $M_Y \leq 1.6$ GeV. Diffractive events are selected by demanding a large empty rapidity gap interval separating the final state hadronic systems X and Y. In another approach the leading final state proton from the process ep → eXp is detected in the H1 Forward Proton Spectrometer. The measurements obtained with the two methods are compared and are also compared with ZEUS measurements. The measurements are compared with predictions from NLO QCD calculations based on diffractive parton densities and from a dipole model.

Key words: diffraction, H1, deep inelastic scattering (DIS), cross-section, large rapidity gap (LRG), forward proton spectrometer (FPS), diffractive structure functions, diffractive parton density function (DPDF), dipole model.

1. INTRODUCTION

Quantum Chromodynamics (QCD) is only able to provide reliable predictions for scattering processes which involve short distance partonic interactions, where perturbative methods may be applied. In contrast, soft interactions to which perturbation theory is not applicable, are dominating hadronic scattering cross sections. In a large fraction of these soft interactions, often termed "diffractive", one or both of the interacting hadrons remains intact. Such processes are commonly discussed in terms of exchanges with net vacuum quantum numbers, though the exact nature of these exchanges is not well known.

* Paper presented at the 8th General Conference of Balkan Physical Union, July 5–7, 2012, Constanta, Romania.

The processes of the type ep → eXY in deep inelastic scattering (DIS) at low Bjorken x at the HERA collider provide a very well controlled environment for studying the QCD properties and structure of diffraction. Here, X is a high-mass hadronic state and Y is the elastically scattered proton or its low-mass excitation, emerging from the interaction with almost the full energy of the incident proton. In contrast to the standard DIS, ep → eX, the diffractive process contains two distinct hadronic final state systems.

The differential diffractive DIS cross section is measured in the kinematic variables of the exchanged boson virtuality Q^2, the inelasticity of the process y, the fraction of the momentum of the proton carried by the diffractive exchange x_{IP} , the Bjorken variable defined for the diffractive exchange β, and the four-momentum transfer squared at the proton vertex |t|. The dependence of diffractive DIS on β, Q^2, x_{IP} and t is studied in terms of the reduced diffractive cross section $\sigma_{\mathrm{r}}^{\mathrm{D(4)}}$. This observable is related to the measured differential cross section,

$$\frac{\mathrm{d}^4\sigma(\mathrm{ep}\to\mathrm{eXp})}{\mathrm{d}\beta\mathrm{d}Q^2\mathrm{d}x_{IP}\mathrm{d}t}=\frac{4\pi\alpha^2}{\beta Q^4}(1-y+\frac{y^2}{2})\cdot\sigma_r^{D(4)}(\beta,Q^2,x_{IP},t). \quad (1)$$

In analogy to the inclusive DIS cross section, in the one-photon exchange approximation, the reduced cross section depends on the diffractive structure functions $F_2^{D(4)}$ and $F_L^{D(4)}$ according to

$$\sigma_r^{D(4)}=F_2^{D(4)}-\frac{y^2}{1+(1-y)^2}F_L^{D(4)}. \quad (2)$$

To a good approximation the reduced cross section is equal to the diffractive structure function $F_2^{D(4)}$ in the region of relatively low y values covered by the H1 diffractive analysis. When the proton is not tagged, an integration over t is performed and $\sigma_r^{D(3)}(\beta,Q^2,x_{IP})$ is measured.

A wide variety of models has been suggested to interpret the dynamics of diffractive DIS as well as its relationships to inclusive DIS and to diffractive hadron-hadron scattering. A general theoretical framework is provided by the QCD collinear factorisation theorem for semi-inclusive DIS cross sections such as that for ep → eXp [1, 2]. This implies that the concept of diffractive parton distribution functions (DPDFs) may be introduced, representing conditional proton parton probability distributions under the constraint of a leading final state proton with a particular four-momentum. Empirically, an additional factorisation has been found to apply to good approximation, whereby the variables which describe the proton vertex factorise from those describing the hard interaction (proton vertex factorisation) [3, 4]. According to this factorisation, the shape of the DPDFs is independent of the four-momentum of the final state proton. The dependence of the DPDF normalisation on the proton four-vector can be parameterized conveniently using Regge formalism which amounts to a description of diffraction in terms of

the exchange of a factorisable 'pomeron' (IP) [5] with universal parton densities. At larger fractional proton energy losses x_{IP} ($x_{IP} > 0.1$), a separately factorisable subleading Reggeon exchange (IR), with a different x_{IP} dependence and partonic composition, is usually included to maintain a good description.

The relationships between the diffractive structure functions and the DPDFs have been shown to be analogous to those of the inclusive case. The diffractive DIS structure function $F_2^{D(4)}$ is then directly sensitive to the singlet quark DPDF and the scaling violations, $\partial F_2^{\mathrm{D}}/\partial \ln Q^2$, provide a measure of the gluon DPDF. As for its inclusive counterpart, F_L^{D} is thus zero in the quark-parton model, but may acquire a non-zero value in QCD, with leading twist contributions dependent on both the diffractive quark and gluon densities [13].

The diffractive cross section can also be interpreted within the dipole model. In this picture, the virtual photon fluctuates into a colour singlet $q\bar{q}$ pair (or dipole) of traverse size $r \sim 1/Q$, which subsequently undergoes a hard scattering with the proton [6–10]. In the domain with low fraction of pomeron momentum carried by the struck parton, β, it is expected that $q\bar{q}$ -g dipoles also contribute to inclusive diffraction [11]. In a recent unified saturation description of diffractive DIS good agreement with data has been obtained in the full range of exchanged with the boson virtuality, Q^2 down to $Q^2 \sim 3$ GeV^2 [12]. This approach is interesting because it relates the diffractive process, in the regime $x_{IP} < 0.01$ in which saturation is expected to be relevant, to the DIS inclusive process.

2. DIFFRACTIVE CROSS SECTION MEASUREMENTS AND MODELS

At high centre-of-mass energy, diffractive ep scattering has two specific signatures. A leading proton carrying most (> 90%) of the beam energy may be directly detected (proton tagging measurement) in the final state using proton spectrometers. Diffraction may also be identified by a final state with no hadronic activity in a large rapidity region, called Large Rapidity Gap (LRG). The LRG separates the outgoing (untagged) proton, or (untagged) low mass hadronic system Y originating from proton dissociation, from the rest of the hadronic system X.

Recently the H1 collaboration finalised measurements of diffractive cross sections obtained with a proton tagged in the Forward Proton Spectrometer FPS [14] and with the LRG method [15] and the results are being reported in this paper. The data are obtained from $e^{\pm}p$ collisions from HERA collider in which electrons or positrons of 27.6 GeV energy collided with 920 GeV protons.

In the LRG analysis the diffractive process $ep \rightarrow eXY$, with a proton or its low mass excitation with $M_Y < 1.6$ GeV, is studied. The analysis is restricted to the phase space region with $3 \leq Q^2 \leq 1600$ GeV^2, $|t| < 1$ GeV^2 and the longitudinal momentum fraction of the incident proton carried by the colourless exchange $x_{IP} < 0.05$. The new measurement is obtained from high statistics data from the 1999–2000 and 2004–2007 periods with a total luminosity of 374 pb^{-1}. The new

result is combined with previously published LRG data (74 pb^{-1}) [16] in order to provide a single set of diffractive cross sections from the H1 experiment using the LGP selection method. The combination is performed using the χ^2 minimisation method developed for the combination of inclusive DIS cross sections [17]. The combined data represent an increase of statistics of a factor between 3 and 30 with respect to the previously published results. With this combination a significant reduction of the statistical and systematic errors is observed. The new combined data have a total uncertainty between 4% and 7% whereas they were typically of the order of 7% and 10% in the previously published results.

The FPS data sample covers the range $x_{IP} < 0.1$ in fractional proton longitudinal momentum loss, $0.1 < |t| < 0.7$ GeV^2 in squared four-momentum transfer at the proton vertex and $4 < Q^2 < 700$ GeV^2 in photon virtuality. From FPS data, the reduced cross section $\sigma_r^{D(3)}(\beta,Q^2,x_{IP})$, defined as the integral of $\sigma_r^{D(4)}(\beta,Q^2,x_{IP},t)$ over t in the range $|t_{min}| < |t| < 1$ GeV^2 is obtained by extrapolating the FPS data from the measured range $0.1 < |t| < 0.7$ GeV^2. The data used in this analysis correspond to an integrated luminosity of 156.6 pb^{-1}.

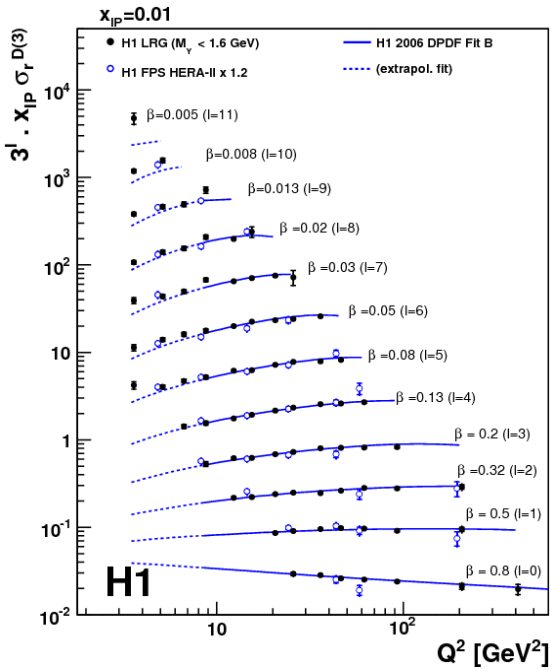

Fig. 1 – The combined H1 LRG data compared with the H1 FPS results. The Q^2 dependence of the reduced diffractive cross section, multiplied by x_{IP}, at fixed value $x_{IP} = 0.01$. The reduced cross section values are multiplied by a scaling factor, 3^l with l values as indicated in parentheses. The inner and outer error bars on the data points represent the statistical and total uncertainties, respectively. The measurements are displaced horizontally for better visibility. Predictions from the H1 2006 DPDF Fit B [16] are represented by a curve in kinematic regions used to determine the DPDFs and by a dashed line in regions which were excluded from the fit (see text).

The cross section ep → eXY measured with the LRG data includes proton dissociation to any system Y with a mass in the range M_Y < 1.6 GeV, whereas in the cross section measured with the FPS the system Y is defined to be a proton. Since the LRG and FPS data sets are statistically independent to a large extent and the dominant sources of systematic errors are different, correlations between the uncertainties on the FPS and LRG data are neglected. The global weighted average of the cross section ratio LRG/FPS is found to be 1.203 ± 0.019 (exp.) ± 0.087 (norm.). The experimental uncertainty of this measurement is a combination of statistical and uncorrelated systematic uncertainties on the measurements. In Fig. 1 the combined LRG cross section measurements as a function of Q^2, for the bin of x_{IP} = 0.01, are compared with the interpolated FPS data rescaled by a factor 1.2. The overall normalisation uncertainties of 4% and 6% on the LRG and FPS data, respectively, are not shown. A good agreement between the two measurements is observed. Figure 1 also shows the prediction from the H1 2006 DPDF Fit B which was based on previously published LRG data from H1 [16]. The DPDF fit assuming proton vertex factorisation used in the previous H1 analysis became unstable when data points with Q^2 < 8.5 GeV^2 were included. Therefore, only an extrapolation of the DPDFs predictions to this kinematic domain is indicated as dashed lines in Fig. 1.

The new combined H1 LRG cross sections are also compared with the most recent measurements by the ZEUS experiment using a similar LRG selection [18]. These ZEUS diffractive data have been determined for identical β and x_{IP} values, but at different Q^2 values to H1. In order to match the M_Y < 1.6 GeV range of the H1 data, a global factor of 0.91 ± 0.07 is applied to the ZEUS LRG data.

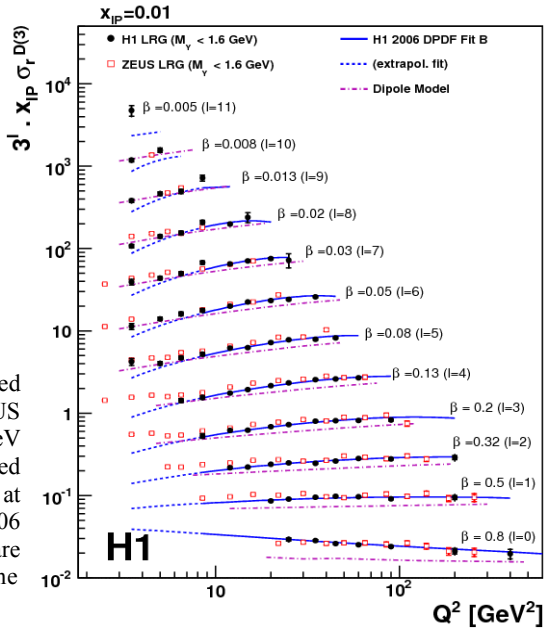

Fig. 2 – The combined H1 LRG data compared with the LRG results of the ZEUS Collaboration [18], corrected to M_Y < 1.6 GeV (see text). The Q^2 dependence of the reduced diffractive cross section multiplied by x_{IP}, at x_{IP} = 0.01. Predictions from the H1 2006 DPDF Fit B [16] and dipole model [12] are displayed. More details are explained in the caption of Fig. 1.

The comparison for $M_Y < 1.6$ GeV between the H1 LRG data and the rescaled ZEUS LRG data is shown in Fig. 2. The ZEUS data tend to remain higher than those of H1 by ~ 10% on average. This difference in normalization is consistent with the 8% uncertainty on the proton-dissociation correction factor of 0.91 ± 0.07 applied to ZEUS data combined with the normalisation uncertainties of the two data sets of 4% (H1) and 2.25% (ZEUS). In Fig. 2 the measurements are compared with predictions based on two models, with the DPDF fit assuming proton vertex factorisation and with dipole model [12]. As the dipole model predictions correspond to the process ep → eXp, they are rescaled by a factor of 1.20. Fig. 2 shows that both approaches give a good overall description of the measurements. In the low Q^2 range, for $Q^2 < 8.5$ GeV^2, the dipole model, which includes saturation effects, seems to better describe the data, whereas for larger β and for $x_{IP} = 0.01$ it tends to underestimate the measured cross section. All the statements made in this section and illustrated with the figures in the bin of $x_{IP} = 0.01$ hold for other x_{IP} bins also.

In Fig. 3 the H1 FPS measurements of $x_{IP}\sigma_r^{D(3)}$ are compared with those of the ZEUS collaboration, measured using their Leading Proton Spectrometer (LPS) [18]. The ratio of the H1 FPS to ZEUS LPS data averaged over the measured kinematic range is $0.85 \pm 0.01(stat.) \pm 0.03(syst.)^{+0.09}_{-0.12}(norm)$ which is consistent with unity taking into account the normalisation uncertainties of 6% and $^{11}_{-7}$% for the H1 FPS and ZEUS LPS data, respectively. Within the errors, there is no strong x_{IP}, or Q^2 dependence of the ratio.

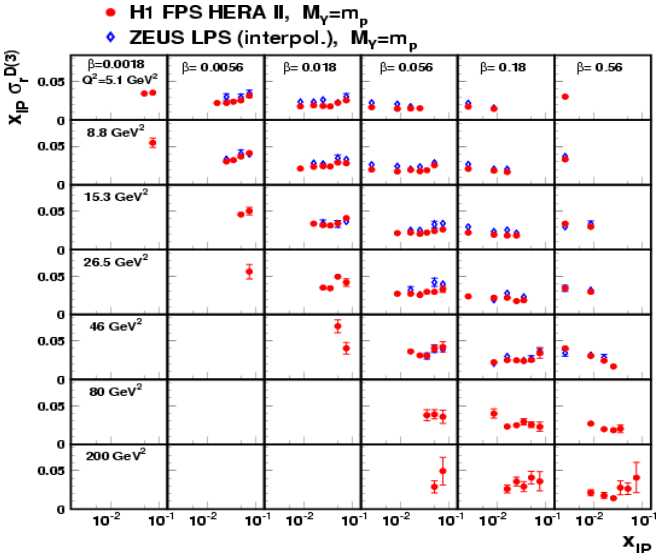

Fig. 3 – The H1 FPS data compared with the ZEUS LPS results [18] interpolated to the FPS β, Q^2, x_{IP} values. The reduced diffractive cross section $x_{IP}\sigma_r^{D(3)}(\beta, Q^2, x_{IP})$ for $|t| < 1$ GeV^2 is shown as a function of x_{IP} for different values of β and Q^2. The error bars indicate the statistical and systematic errors added in quadrature.

3. COMPARISON BETWEEN DIFRACTIVE AND INCLUSIVE DIS

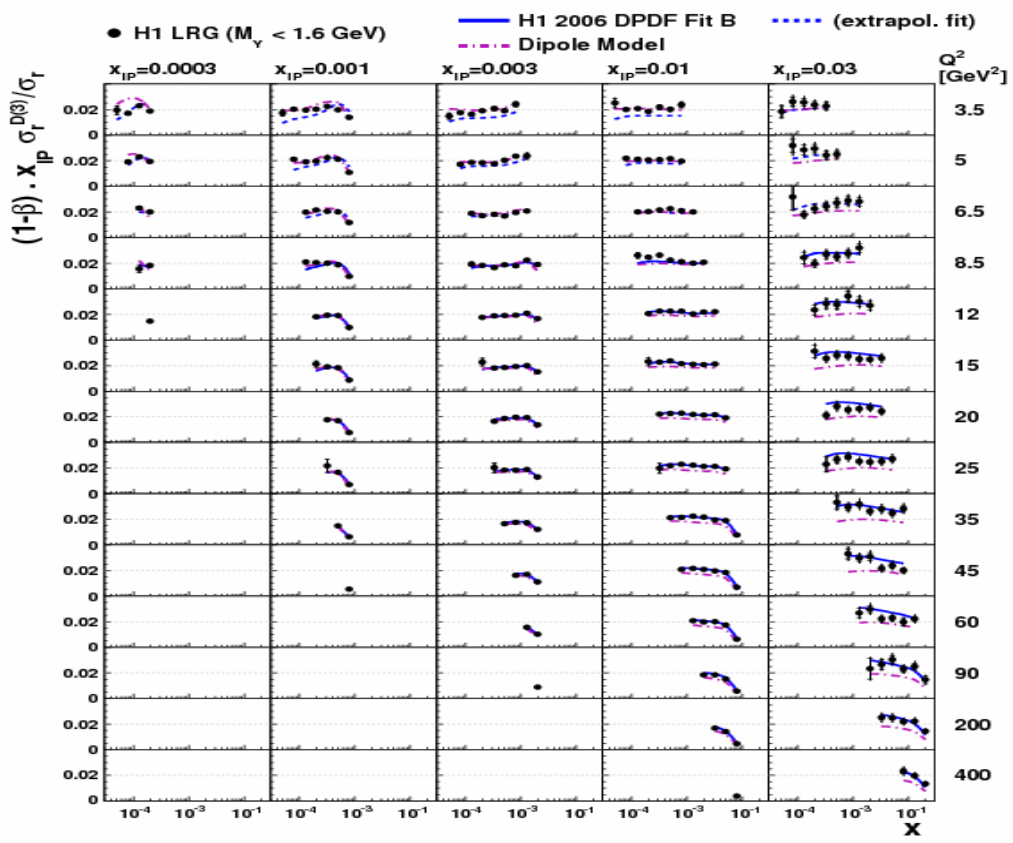

Fig. 4 – The ratio of the LRG diffractive to the inclusive reduced cross section, multiplied by $(1–\beta)x_{IP}$. The curves are explained in the captions of Figs. 1 and 2.

The comparison of Q^2 and x dynamics of the diffractive with the inclusive cross section can improve our understanding of high energy QCD, comparing the properties of diffractive PDFs with their inclusive counterparts and testing models. Following [16], the evolution of the diffractive reduced cross section with Q^2 is compared with that of the inclusive DIS reduced cross section by forming the ratio $\sigma_r^{D(3)}(x_{IP},\beta,Q^2)/\sigma_r(x=\beta x_{IP},Q^2)$ multiplied by $(1–\beta)x_{IP}$ at fixed Q^2,β and x_{IP}, using a parameterisation of the σ_r data from [19]. The ratio of the diffractive LRG to the inclusive cross section is shown in Fig. 4 as a function of x at fixed x_{IP} and Q^2 values. This ratio is found to be approximately constant with x at fixed Q^2 and x_{IP} except towards larger x values which correspond to large β values. This indicates that the ratio of quark to gluon distributions is similar in the diffractive and inclusive process when considered at the same low x value. The ratio is also larger

at high values of x_{IP}, $x_{IP} = 0.03$, where the sub-leading exchange contribution of the diffractive cross section is not negligible, but it remains approximately constant with x. The same conclusion is obtained from the FPS data [14].

4. EXTRACTION OF THE POMERON TRAJECTORY

The diffractive structure function $F_2^{D(3)}$ can be investigated in the framework of Regge phenomenology and is usually expressed as a sum of two factorised contributions corresponding to Pomeron and secondary Reggeon trajectories,

$$F_2^{D(3)}(Q^2, \beta, x_{IP}) = f_{IP/p}(x_{IP}) F_2^{IP}(Q^2, \beta) + n_{IR} f_{IR/p}(x_{IP}) F_2^{IR}(Q^2, \beta). \quad (3)$$

Here, F_2^{IP} can be interpreted as the Pomeron structure function and F_2^{IR} as an effective Reggeon structure function. n_{IR} is the global normalisation of this last contribution. The Pomeron and Reggeon fluxes are assumed to follow a Regge behaviour with linear trajectories $\alpha_{IP,IR}(t) = \alpha_{IP,IR}(0) + \alpha_{IP,IR} t$, such that

$$f_{IP/p,iR/p}(X_{IP}) = \int_{t_{cut}}^{t_{min}} \frac{e^{B_{IP,IR} t}}{X_{IP}^{2\alpha_{IP,IR}(t)-1}} \mathrm{d}t \quad (4)$$

$|t_{min}|$ is the minimum kinematically allowed value of $|t|$ and $t_{cut} = -1$ GeV is the limit of the measurement.

The diffractive structure function $F_2^{D(3)}$ is obtained from the reduced cross section by correcting for the small contribution from $F_L^{D(3)}$ using the predictions of the H1 2006 DPDF Fit B, which is in reasonable agreement with the recent direct measurement of $F_L^{D(3)}$ [19].

In both, FPS and LRG analyses, fitting the form of equation 3 to the experimental $F_2^{D(3)}$ data, the free parameters in the fit are: the intercept, $\alpha_{IP}(0)$, the Pomeron structure function $F_{IP}(\beta, Q^2)$ at each of the (β, Q^2) values, and the single parameter n_{IR}. In the FPS analysis the pomeron trajectory, α'_{IP}, and exponential t-slope parameter B_{IP} were free parameters and are also determined from the fit. The obtained values are fixed in LRG analysis. The values of the other parameters are fixed in the fit and used from other publications (for more details see [14, 15]). The full range in Q^2 is divided in several intervals. For each interval, a free Pomeron intercept is introduced, so the factorisation assumption can be tested differentially in Q^2. In the minimisation procedure the error of each data points is obtained by adding in quadrature the statistical and uncorrelated systematic uncertainties. The effect of correlated uncertainties is taken into account by repeating of the fit multiple times with each correlated systematic error shifted by one standard deviation. The results on the Pomeron intercept are presented in Fig. 5. From this

figure, one sees no significant Q^2 dependence of the Pomeron intercept which supports the proton vertex factorization hypothesis. The averaged measured value obtained in the LRG analysis is $\alpha_{IP}(0) = 1.113 \pm 0.002(\text{exp.})^{+0.029}_{-0.015}(\text{model})$. The new measurements at the H1 are in good agreement with previous H1 and recent ZEUS determinations [16, 18].

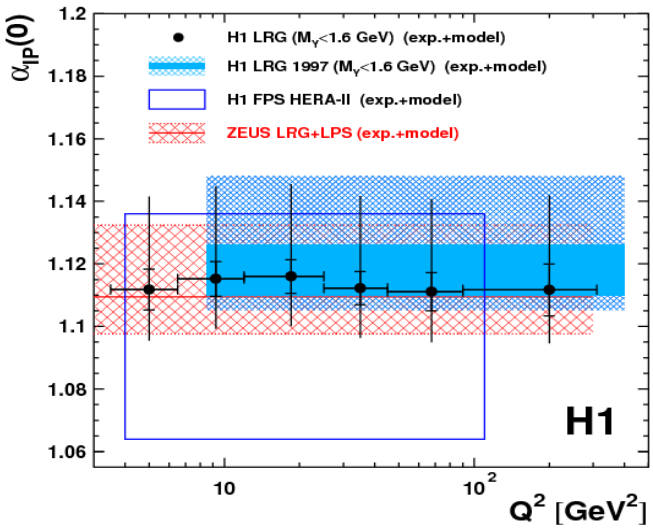

Fig. 5 – Pomeron intercept values obtained from Regge fits in different Q^2 bins. For the combined H1 LRG data the inner error bars represent the statistical and systematic errors added in quadrature and the outer error bars include model uncertainties in addition. For the other measurements shown the bands or boxes represent the combination of experimental and model uncertainties, always dominated by the model error.

5. CONCLUSIONS

The full H1 data sample has been analysed to measure diffractive DIS cross section by requiring the presence of a large rapidity gap or by using the Forward Proton Spectrometer for the detection of the leading final state proton. By comparing to the proton-tagged cross section measurements, a contribution of 20% of proton dissociation is found to be present in the large rapidity gap data. The two measurements are found to be in good agreement in the common phase space. H1 measurements obtained by various methods are compared with those obtained from ZEUS and all measurements are found to be consistent throughout most of the phase space. The new H1 diffractive cross section measurements are also compared with predictions from dipole and DPDF approaches. A reasonable description of the data is achieved by both models. The predictions of the dipole model, including

saturation, can describe the low Q^2 kinematic domain of the measurements better than the previous H1 DPDF fits.

The ratio of quark to gluon distributions is similar in the diffractive and inclusive process when considered at the same low x value. This follows from the ratio of the diffractive to the inclusive ep cross section which is measured as a function of x, Q^2 and x_{IP}. At fixed x_{IP} the ratio depends only weakly on x, except at the highest x values.

A possible Q^2 dependence of the Pomeron intercept was tested and it was shown that the results do not exhibit any dependence on Q^2 which is compatible with previous determinations and supports the proton vertex factorisation hypothesis.

Acknowledgments. I thank all colleagues from H1 collaboration who contributed in obtaining the results presented here, especially to Emmanuel Sauvan, Laurent Schoeffel and Mikhail Kapichine.

REFERENCES

1. J. Collins, Phys. Rev., **D 57**, 3051 (1998).
2. L. Trentadue and G. Veneziano, Phys. Lett., **B 323**, 201 (1994).
3. G. Ingelman and P. Schlein, Phys. Lett., **B 152**, 256 (1985).
4. A. Donnachie and P. Landshoff, Phys. Lett., **B 191**, 309 (1987).
5. E. Feinberg and I. Pomeranchuk, Suppl. Nuovo. Cimento., **3**, 652 (1956); V. Gribov, JETP Lett., **41**, 667 (1961).
6. A. H. Mueller, Nucl. Phys., **B 335**, 115 (1990).
7. N. N. Nikolaev and B. G. Zakharov, Z. Phys., **C 49**, 607 (1991).
8. E. Iancu, K. Itakura and S. Munier, Phys. Lett., **B 590**, 199 (2004).
9. K. Golec-Biernat and M. W¨usthoff, Phys. Rev., **D 59**, 014017 (1999).
10. C. Marquet and L. Schoeffel, Phys. Lett., **B 639**, 471 (2006).
11. K. J. Golec-Biernat and M. Wusthoff, Phys. Rev., **D 60**, 114023 (1999).
12. C. Marquet, Phys. Rev., **D 76**, 094017 (2007).
13. A. Zee, F. Wilczek and S. B. Treiman, Phys. Rev., **D 10**, 2881 (1974); G. Altarelli and G. Martinelli, Phys. Lett., **B 76**, 89 (1978).
14. F. D. Aaron et al. [H1 Collaboration], Eur. Phys. J., **C 71**, 1578 (2011).
15. F. D. Aaron et al. [H1 Collaboration], arxiv:1203.4495.
16. A. Aktas et al. [H1 Collaboration], Eur. Phys. J., **C 48**, 715 (2006).
17. A. Glazov, AIP Conf. Proc. **792**, 237 (2005).
18. S. Chekanov et al. [ZEUS Collaboration], Nucl. Phys., **B 816**, 1 (2009).
19. F. D. Aaron et al. [H1 Collaboration], Eur. Phys., J. **C 64**, 561 (2009).
20. F. D. Aaron et al. [H1 Collaboration], Eur.Phys.J., **C 72**, 1836 (2012).